Hindawi
Advances in Civil Engineering
Volume 2020, Article ID 6625940, 11 pages
https://doi.org/10.1155/2020/6625940

Research Article

Study on Identification of Construction Method for Ultra-Large-Span Tunnel

Xu Chongbang [1,2,3] and Qin Youlin [1,2,3]

[1]*Bridge and Tunnel Research Center, Research Institute of Highway Ministry Transport, Beijing 100088, China*
[2]*National Engineering Laboratory of Bridge Sructure Safety Technology, Beijing 100088, China*
[3]*Research Institute of Highway Ministry of Transport Research and Development Center of Transport Industry of Technologies and Equipments for Intelligent Design, Construction and Maintenance of Underwater Tunnel, Ministry of Transport, Beijing 100088, China*

Correspondence should be addressed to Xu Chongbang; xubang-2003@163.com

Received 10 October 2020; Revised 5 December 2020; Accepted 14 December 2020; Published 24 December 2020

Academic Editor: Zhi Cheng Tang

Although the determination of tunnel construction methods is extremely critical for the construction of ultra-large-span tunnels, the determination of construction methods is still at a qualitative level, which relies on the engineering experience of on-site technicians and lacks rigorous and systematic theoretical basis and technical standards. By means of orthogonal test method, the proper construction method was established for the deep-buried ultra-large-span tunnel where the tunnel excavation span, tunnel surrounding rock strength, and rock integrity coefficient were set as the main control factors. The stability of tunnel surrounding rock under various test conditions was quantified according to the plastic zone properties calculated by the three-factor and five-level orthogonal test model. Meanwhile, the macro form and quantitative method of test combinations under different levels of various factors were proposed to obtain the influence of each factor on the stability of tunnel surrounding rock, and thus the functional relations between various factors and tunnel stability were obtained. On this basis, the identification and the criterion of the ultra-large-span tunnel construction method were established, which can quantitatively reflect the contribution of excavation span of the tunnel, the number of lateral drifts in cross section, surrounding rock strength, and rock integrity coefficient to surrounding rock stability of the tunnel. The construction method calculation results of the Malin tunnel, a practical underground project, are obtained according to the orthogonal test model calculation. Based on the method, Malin tunnel can be constructed safely and efficiently. The research results could provide the theoretical basis for the identification and selection of construction method for ultra-large-span tunnel.

1. Introduction

The determination of tunnel construction methods is extremely critical for the construction of ultra-large-span tunnels, which directly affects the construction safety, progress, costs, and the configuration of humans, machines, and materials during construction. Various methods for ultra-large-span tunnel construction have been developed under the influences of many factors including the size of the tunnel section and topographical, engineering geological, and hydrogeological conditions. The commonly used methods include the center diaphragm method (CD method) [1], center cross diagram method (CRD) [2–6], the double-side drift method [7–9] and the three-stage and seven-step method [10, 11], and other methods derived from these basic methods. In the construction of ultra-large-span tunnels, the determination of construction methods is still at a qualitative level, which relies on the engineering experience of on-site technicians and lacks rigorous and systematic theoretical basis and related technical standards [12].

In common practices, factors considered during selecting construction methods often include (1) project factors, such as overall excavation span of the tunnel, the maximum single excavation span, and auxiliary engineering measures [13], and

(2) geological and environmental factors, such as the properties of surrounding rock (the strength of the surrounding rock and the integrity coefficient of the rock mass) [14–19], groundwater [20], and the in situ stress [21]. In order to ensure the stability of the tunnel after blasting and before the initial support construction, the maximum one-step excavation span of the tunnel, the strength of the surrounding rock, and rock integrity are placed at the top priority. Other factors are generally considered as supplementary grounds for final decision. In this paper, we established the orthogonal test model to determine the proper construction method for the deep-buried ultra-large-span tunnel where the tunnel excavation span, tunnel surrounding rock strength, and rock integrity coefficient were set as the main control factors. Our work aims to establish the evaluation system for selection of construction method and provide theoretical calculation basis for determining the number of lateral drifts in cross section of ultra-large-span tunnels through the quantification of control factors on the stability of surrounding rock during tunnel excavation.

2. Orthogonal Test Design

2.1. The Level of Orthogonal Factors. In order to elucidate the influence of tunnel span, surrounding rock strength, and rock integrity coefficient on the stability of tunnel surrounding rock, a five-level orthogonal test scheme is designed in this paper. The tunnel span, surrounding rock strength, and rock integrity coefficient are represented by A, B, and C, respectively. The five levels of the three factors are set as follows:

(1) Factor A: with reference to the drift span, common tunnel span, and ultra-large-span tunnel span in highway tunnels, the five levels of factor A are designed as 6 m, 9 m, 12 m, 15 m, and 18 m, and the tunnel cross section is shown in Figure 1.

(2) Factor B: factor B is the rock strength, which is divided according to the degree of soft and hard rock. The five levels of factor B are designed as 2 MPa, 10 MPa, 20 MPa, 40 MPa, and 65 MPa. According to the Mohr–Coulomb criterion, the internal friction angle φ and cohesive force C corresponding to the five levels are listed in Table 1.

(3) Factor C: the five levels of factor C, which represents the coefficient of surrounding rock integrity, are 0.1, 0.2, 0.4, 0.6, and 0.75. The five levels of factor C in the test are shown in Table 2. The test parameters of the joint plane are selected in accordance with the recommended values of the peak shear strength of the rock discontinuity structural plane in the "Road Tunnel Design Rules" [22], as listed in Table 3.

2.2. Orthogonal Test Combinations. According to the orthogonal test design [23], the three-factor and five-level orthogonal test requires a total of 25 tests. The combinations of orthogonal tests are shown in Table 4:

3. Calculations and Results

3.1. Model Size. In order to eliminate the boundary effect of the tunnel calculation model, the size of the model was determined as 200 m (width) × 110 m (height). The buried depth of the tunnel was set as 50 m, as the typical depth of deep-buried tunnel. The tunnel structure was placed in the center of the model (Figure 2). The simulated tunnel construction employed a one-step excavation method without considering the role of lining support structure. The stress release rate of the tunnel surrounding rock was defined as 30%.

3.2. Criterion of Surrounding Rock Instability. In the experimental calculation model, the surrounding rock was assumed as ideal elastoplastic material, and thus the Mohr–Coulomb constitutive model was used to develop the criterion of surrounding rock instability [22] based on "Road Tunnel Design Rules." It is assumed that the surrounding rock becomes unstable when plastic zones appear in the surrounding rock at the tunnel arch and the side walls and these zones communicate with each other. Meanwhile, in order to quantify the stability of the tunnel under each simulated condition, the properties of the plastic zone were quantified according to Table 5.

3.3. Calculation Results

3.3.1. Example of Surrounding Rock Stability Analysis. Here no. 1 A1B1C1 is taken as an example to illustrate the analysis process of surrounding rock stability. In the no. 1 test, there are multiple tensile stress distribution areas in the tunnel vault and arch wall (Figure 3). Plastic zones are found at the joint planes and rock blocks of the tunnel arch and the side walls, which connect each other (Figure 4). Therefore, it can be concluded that the full-face excavation under this three-factor combination is unstable. The quantitative score of the no. 1 test is 1 point.

3.3.2. Test Results. According to the conditions of the plastic zone calculated from the 25 sets of experiments, the results of the experimental calculations were quantified according to the quantitative rules. The quantitative statistical results and the tunnel stability are listed in Table 6.

4. Identification of Construction Method for Ultra-Large-Span Tunnel

4.1. Data Processing. In order to quantitatively analyze the influence of a single factor on the stability of the tunnel, the test data of each group were processed in combinations from a macro perspective to eliminate the impact of other factors based on the same frequency and probability of each level of every factor in the orthogonal test. Factor A is used as an example to explain the detailed process.

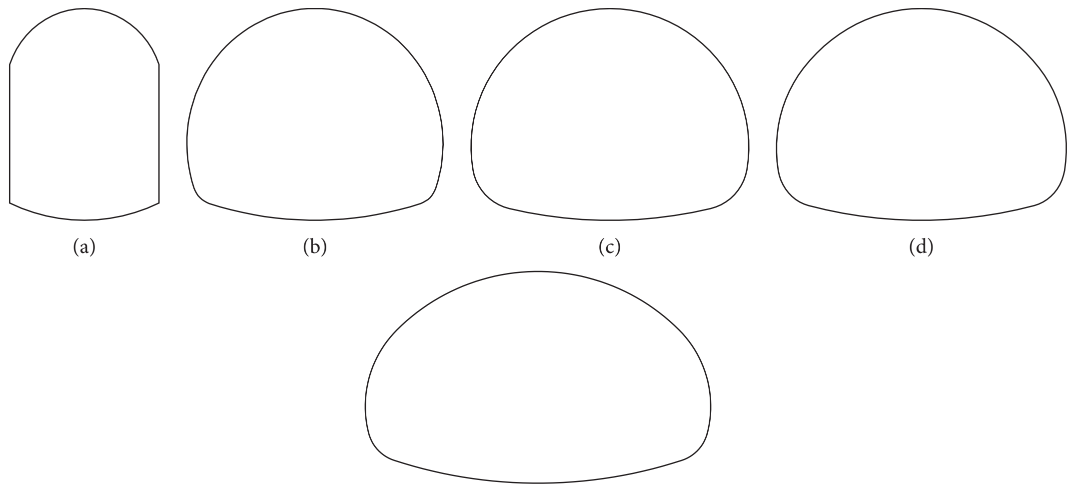

Figure 1: Five types of tunnel cross section. (a) With span of 6 m. (b) With span of 9 m. (c) With span of 12 m. (d) With span of 15 m. (e) With span of 18 m.

Table 1: Parameter values of each level of factor A.

Level	Compressive strength (MPa)	Internal friction angle φ (°)	Cohesive force C (MPa)	Volumetric weight γ ($kN \cdot m^{-3}$)	Elasticity modulus E (GPa)	Poisson's ratio μ
1	2	27.5	1.6	22	1.0	0.3
2	10	37	2.5	22	1.0	0.3
3	20	46.4	4	22	1.0	0.3
4	40	56.6	6	22	1.0	0.3
5	65	63	7.8	22	1.0	0.3

Note. The influences of volumetric weight, elasticity modulus, and Poisson's ratio were not considered.

Table 2: Parameter values of each level of factor C.

Level	Number of joint planes	Space of joint plane	Joint inclination angle (°)	Coefficient of surrounding rock integrity
1	4	0.2	0/90/45/135	0.1
2	3	0.3	0/90/45	0.2
3	2	0.4	0/90	0.4
4	2	0.8	0/90	0.6
5	2	1.5	0/90	0.75

Table 3: Joint plane parameters.

Internal friction angle φ (°)	Cohesive force C (MPa)	Compressive strength (MPa)
15	0.06	0.13

4.1.1. Combination of Test Conditions. The levels of factor A are the main study targets. Combining the levels of factor A with the five levels of factor B and factor C obtains the macro form of the test combinations (Table 7). The obtained combinations have the same macro combination of factor B and factor C for each level of factor A. Therefore, on this basis, comparative analysis of the influence of various levels of factor A on tunnel stability can be performed.

4.1.2. Quantification of the Macro Form of the Test Combinations. In order to quantify the influence of various factors on the tunnel stability, it is necessary to quantify the macro form of the test combinations. Given that the conditions under the combination are all independent, the linear superposition method is used to define the quantitative scores of factor A under each level to obtain the quantitative index F of tunnel stability under different combinations. The detailed calculation process is as follows:

(a) The first level of factor A (6 m span): IA = A1B(5) C(5) = 1 + 2 + 5 + 6 + 6 = 20.

(b) The second level of factor A (9 m span): IIA = A2B(5) C(5) = 1 + 3 + 5 + 5 +3 = 17.

(c) The third level of factor A (12 m span): IIIA = A3B(5) C(5) = 1 + 3 + 5 + 3+ 4 = 16.

Table 4: Orthogonal test analysis.

No.	Excavation span *A*	Surrounding rock strength *B*	Coefficient of surrounding rock integrity *C*	Code
1	1 (6 m)	1 (2 MPa)	1 (0.1)	A1B1C1
2	1 (6 m)	2 (10 MPa)	2 (0.2)	A1B2C2
3	1 (6 m)	3 (20 MPa)	3 (0.4)	A1B3C3
4	1 (6 m)	4 (40 MPa)	4 (0.6)	A1B4C4
5	1 (6 m)	5 (65 MPa)	5 (0.75)	A1B5C5
6	2 (9 m)	1 (2 MPa)	2 (0.2)	A2B1C2
7	2 (9 m)	2 (10 MPa)	3 (0.4)	A2B2C3
8	2 (9 m)	3 (20 MPa)	4 (0.6)	A2B3C4
9	2 (9 m)	4 (40 MPa)	5 (0.75)	A2B4C5
10	2 (9 m)	5 (65 MPa)	1 (0.1)	A2B5C1
11	3 (12 m)	1 (2 MPa)	3 (0.4)	A3B1C3
12	3 (12 m)	2 (10 MPa)	4 (0.6)	A3B2C4
13	3 (12 m)	3 (20 MPa)	5 (0.75)	A3B3C5
14	3 (12 m)	4 (40 MPa)	1 (0.1)	A3B4C1
15	3 (12 m)	5 (65 MPa)	2 (0.2)	A3B5C2
16	4 (15 m)	1 (2 MPa)	4 (0.6)	A4B1C4
17	4 (15 m)	2 (10 MPa)	5 (0.75)	A4B2C5
18	4 (15 m)	3 (20 MPa)	1 (0.1)	A4B3C1
19	4 (15 m)	4 (40 MPa)	2 (0.2)	A4B4C2
20	4 (15 m)	5 (65 MPa)	3 (0.4)	A4B5C3
21	5 (18 m)	1 (2 MPa)	5 (0.75)	A5B1C5
22	5 (18 m)	2 (10 MPa)	1 (0.1)	A5B2C1
23	5 (18 m)	3 (20 MPa)	2 (0.2)	A5B3C2
24	5 (18 m)	4 (40 MPa)	3 (0.4)	A5B4C3
25	5 (18 m)	5 (65 MPa)	4 (0.6)	A5B5C4

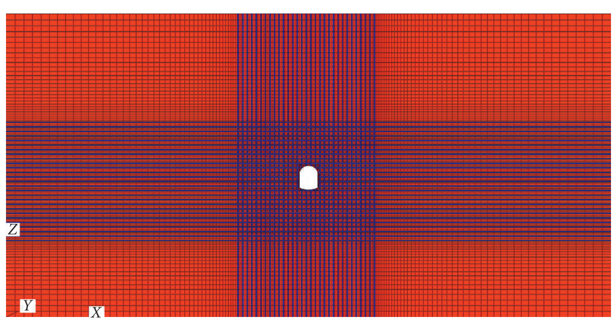

Figure 2: Calculation model of no. 1 test.

Table 5: Criterion and quantitative standard of surrounding rock stability state.

No.	Conditions of the plastic zone	Stability of surrounding rock	Quantitative score
1	Communicated plastic zones occur in both joint planes and rock blocks	Unstable	1
2	Plastic zones occur in both joint planes and rock blocks, but only communicate in joint planes	Unstable	2
3	Communicated plastic zones only occur in joint planes	Unstable	3
4	Noncommunicated plastic zones occur in both joint planes and rock blocks	Stable	4
5	Noncommunicated plastic zones occur in joint planes	Stable	5
6	No plastic zones occur in both joint planes and rock blocks	Stable	6

(d) The fourth level of factor A (15 m span): IVA = A4B(5)C(5) = 1 + 3 + 1 + 3 +5 = 13.

(e) The fifth level of factor A (18 m span): VA = A5B(5) C(5) = 2 + 1 + 2 + 3 + 5 = 13.

4.1.3. Processing Results. The data processing of factors B and C is carried out in the same way, and their quantitative index F under various levels is calculated, as listed in Table 8.

As indicated by the range of the stability quantitative index of three factors in Table 8 [24], the strength of the

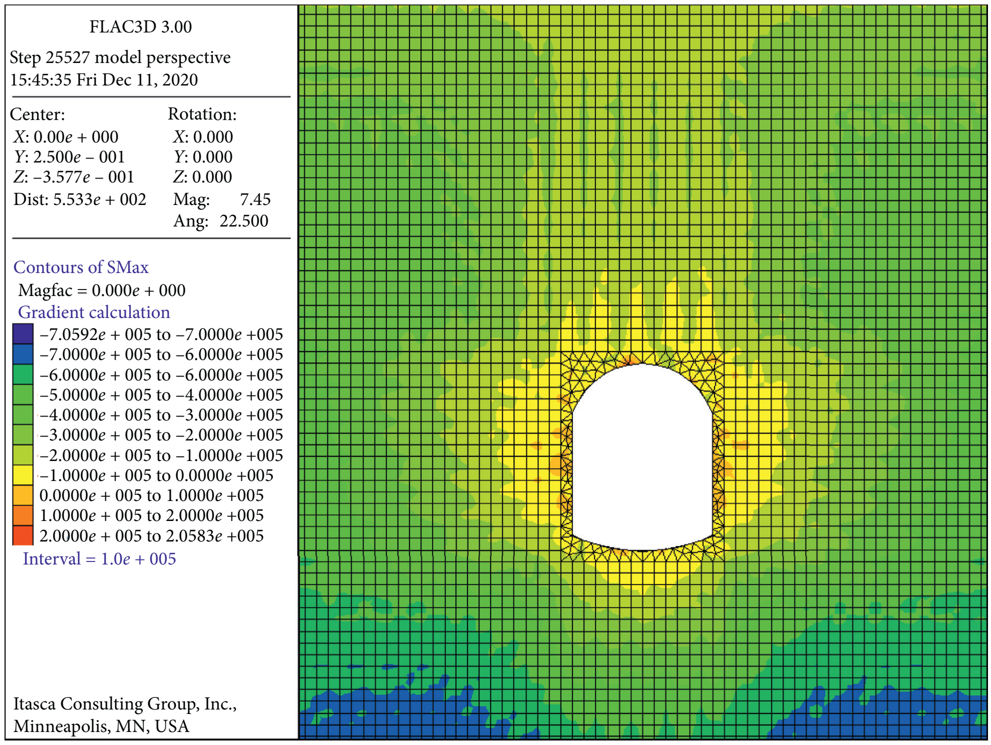

Figure 3: Principal stress distribution of surrounding rock.

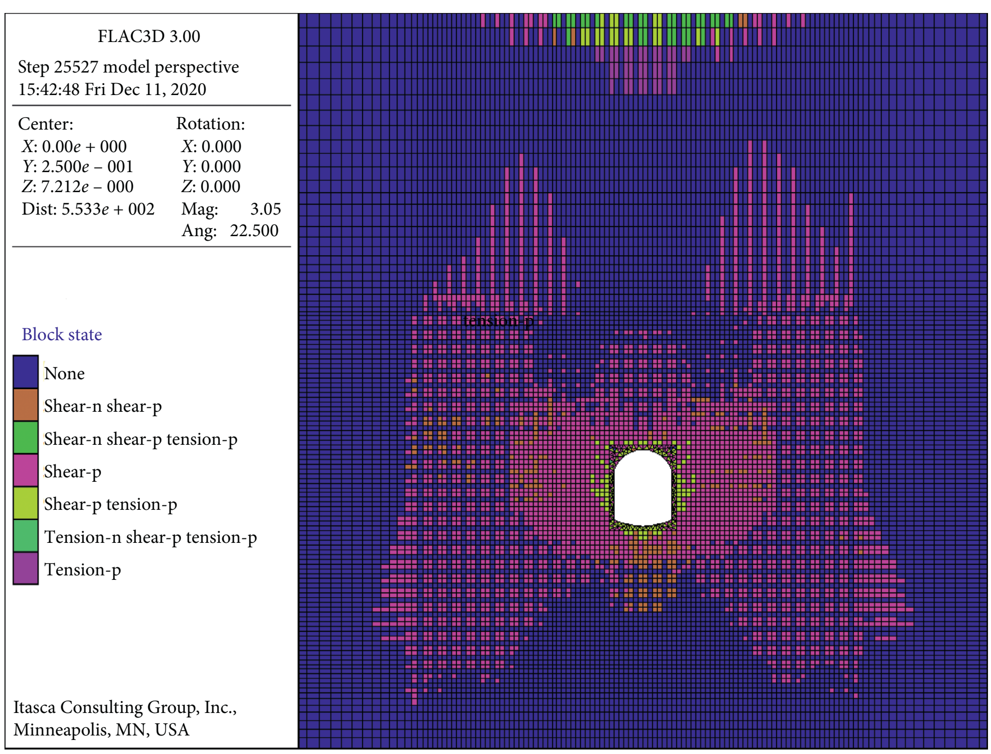

Figure 4: Distribution of plastic zone of surrounding rock.

Table 6: Quantification of test data and stability index.

Test no.	Test code	Stability	Quantitative score
1	A1B1C1	Unstable	1
2	A1B2C2	Unstable	2
3	A1B3C3	Stable	5
4	A1B4C4	Stable	6
5	A1B5C5	Stable	6
6	A2B1C2	Unstable	1
7	A2B2C3	Unstable	3
8	A2B3C4	Stable	5
9	A2B4C5	Stable	5
10	A2B5C1	Unstable	3
11	A3B1C3	Unstable	1
12	A3B2C4	Unstable	3
13	A3B3C5	Stable	5
14	A3B4C1	Unstable	3
15	A3B5C2	Stable	4
16	A4B1C4	Unstable	1
17	A4B2C5	Unstable	3
18	A4B3C1	Unstable	1
19	A4B4C2	Unstable	3
20	A4B5C3	Stable	5
21	A5B1C5	Unstable	2
22	A5B2C1	Unstable	1
23	A5B3C2	Unstable	2
24	A5B4C3	Unstable	3
25	A5B5C4	Stable	5

Table 7: Macro form of test combination at each level of factor A.

No.	Excavation span (A)	Code of test combinations	Macro form of the test combinations
1	1	A1B1C1、A1B2C2、A1B3C3、A1B4C4、A1B5C5	A1B(5)C(5)
2	2	A2B1C2、A2B2C3、A2B3C4、A2B4C5、A2B5C1	A2B(5)C(5)
3	3	A3B1C3、A3B2C4、A3B3C5、A3B4C1、A3B5C2	A3B(5)C(5)
4	4	A4B1C4、A4B2C5、A4B3C1、A4B4C2、A4B5C3	A4B(5)C(5)
5	5	A5B1C5、A5B2C1、A5B3C2、A5B4C3、A5B5C4	A5B(5)C(5)

Note. B(5) represents the combinations of five levels of factor B and C(5) represents the combinations of five levels of factor C.

Table 8: Quantitative index value of tunnel stability under different factor levels.

Level of factor	Quantitative index value of tunnel stability F		
	Tunnel span A	Rock strength B	Coefficient of rock integrity C
I	20	6	9
II	17	12	12
III	16	18	17
IV	13	20	20
V	13	23	21
Range	7	17	12

surrounding rock has the most significant impact on tunnel stability, followed by the surrounding rock integrity and the span of the tunnel in decreasing order.

4.2. The Influence of Main Control Factors on Tunnel Stability. Based on the stability quantitative index of three factors listed in Table 8, the influence rule of these factors on tunnel stability can be drawn, as shown in Figures 5–7, respectively.

4.2.1. Tunnel Span. According to Figure 5, the tunnel excavation span has a negative correlation with the stability of the surrounding rock. The stability of the tunnel deteriorates with the increase of tunnel span. The relationship between them is expressed as a power function:

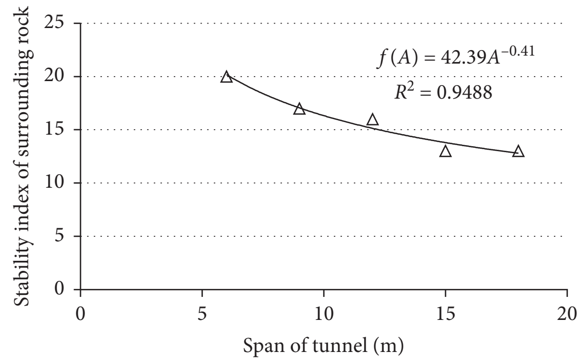

Figure 5: Fitting curve between stability index of surrounding rock and span of tunnel.

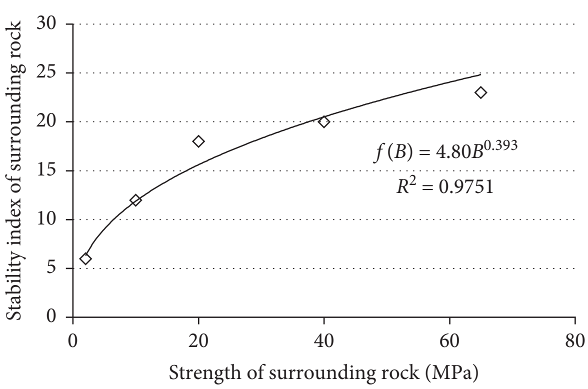

Figure 6: Fitting curve between stability index and strength of surrounding rock.

$$f(A) = 42.39A^{-0.41}. \quad (1)$$

4.2.2. Compressive Strength of Surrounding Rock. Figure 6 shows a strong positive correlation between surrounding rock strength and tunnel stability. A higher compressive strength of surrounding rock is beneficial for better tunnel stability. Their relation can be expressed as

$$f(B) = 4.80B^{0.393}. \quad (2)$$

4.2.3. Coefficient of Surrounding Rock Integrity. The tunnel stability is positively related with the coefficient of surrounding rock integrity, indicating that higher coefficient of surrounding rock integrity contributes to tunnel stability. The relation can be expressed as

$$f(C) = 6.208\ln(C) + 22.78, \quad (3)$$

where $f(C) > 0$; therefore, the coefficient of surrounding rock C should be greater than 0.03.

4.3. The Expression of Quantitative Index of Surrounding Rock Stability. The stability of the surrounding rock of the tunnel is the result of the combined action of the three main control

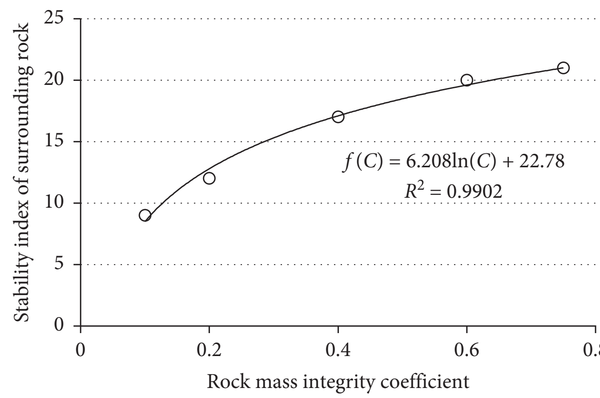

Figure 7: Fitting curve between stability index of surrounding rock and rock mass integrity coefficient.

factors. The influences of the main control factors on the stability are interrelated and coupled. This correlation can be expressed by their product and a coefficient k. Therefore, the tunnel stability after excavation can be quantified as

$$F = kf(A)f(B)f(C). \quad (4)$$

Substituting equations (1)–(3) into equation (4), F can be derived:

$$F = A^{-0.41}B^{0.393}(6.208\ln(C) + 22.78), \quad (5)$$

where k is a constant value ($k = 0.004907$).

4.4. Criterion of Quantification of Surrounding Rock Stability. Substituting the test calculation parameters (Table 4) into equation (5), the value of the tunnel stability quantitative index F for each test can be obtained (Table 9).

It can be seen from Table 9 that in 25 sets of orthogonal tests, the minimum index is 5.3 and the maximum is 22.3 when the surrounding rock is unstable after tunnel excavation. And the minimum index is 23.8 and the maximum is 51.9 when the surrounding rock of the tunnel remains stable. Therefore, the criteria for stability of surrounding rock can be given as follows:

(1) If $F \geq 23$, the surrounding rock is in stable sate.

(2) If $F < 23$, the surrounding rock becomes unstable.

According to this criterion and the quantification rules, the stability index F can be classified as six levels specifically, as listed in Table 10.

4.5. Criterion for Tunnel Construction Method Selection

4.5.1. One-Step Maximum Excavation Span. According to equation (5), for a given tunnel surrounding rock, a proper one-step excavation span should be selected to satisfy the index $F \geq 23$ to ensure the stability of the surrounding rock during excavation. Thus, maximum span A_{max} of the next-step excavation can be calculated under given surrounding rock properties (strength and integrity coefficient) when assuming that $F = 23$, as shown in the following equation:

Table 9: Index calculation value of tunnel stability.

Test no.	Test code	Stability	*F*
1	A1B1C1	Unstable	5.3
22	A5B2C1	Unstable	6.4
6	A2B1C2	Unstable	6.8
11	A3B1C3	Unstable	8.1
21	A5B1C5	Unstable	8.4
16	A4B1C4	Unstable	8.5
18	A4B3C1	Unstable	9.1
23	A5B3C2	Unstable	12.7
14	A3B4C1	Unstable	13.1
2	A1B2C2	Unstable	15.2
17	A4B2C5	Unstable	17.1
7	A2B2C3	Unstable	17.2
12	A3B2C4	Unstable	17.5
10	A2B5C1	Unstable	17.8
19	A4B4C2	Unstable	18
24	A5B4C3	Unstable	22.3
15	A3B5C2	Stable	23.8
13	A3B3C5	Stable	24.6
8	A2B3C4	Stable	25.9
3	A1B3C3	Stable	26.6
20	A4B5C3	Stable	29
25	A5B5C4	Stable	30.9
9	A2B4C5	Stable	36.3
4	A1B4C4	Stable	40.1
5	A1B5C5	Stable	51.9

Table 10: Index value and qualitative description of tunnel stability.

F	Unstable state			Stable state		
	<13	[13, 17)	[17, 23)	[23, 26)	[26, 40)	≥40
Description of stability	Extremely unstable	Very unstable	Unstable	Basically stable	Very stable	Highly stable

$$A_{\max} = \left(\frac{B^{0.393} \left(6.208 \ln (C) + 22.78 \right)}{23} \right)^{2.44}. \tag{6}$$

4.5.2. Determination of the Number of Drifts. Assuming that the maximum span of tunnel excavation is L and the number of lateral drifts in the cross section is N, it can be seen from equation (6) that the number of lateral drifts in the tunnel section should be

$$N \geq \frac{L}{A_{\max}} = \frac{L}{\left(\left(B^{0.393} \left(6.208 \ln (C) + 22.78 \right) \right) / 23 \right)^{2.44}}. \tag{7}$$

Thus,

$$N_{\min} = \frac{L}{\left(\left(B^{0.393} \left(6.208 \ln (C) + 22.78 \right) \right) / 23 \right)^{2.44}}, \tag{8}$$

where $N_{\min}$ should be integer.

4.5.3. Bench Division of Tunnel Drift. After determining the number of lateral drifts, the stability state of the tunnel drift is used as a reference for the necessity of bench cut. It is recommended to perform bench cut construction in the lateral drifts as instructed by Table 11.

4.6. Influencing Analysis of Other Factors. In the construction phase of tunnel engineering, the identification of construction method should consider not only the three crucial factors including tunnel span, rock mass integrity coefficient, and strength of surrounding rock but also the secondary factors such as in situ stress, groundwater, and construction capacity of the subcontractors. The secondary influence factors are restricted by the geological conditions of the tunnel site, which is not universal. Therefore, in the actual tunnel projects, the influence of secondary factors can be revised according to the specific situation of projects, and the influence of secondary factors is reflected by means of revision.

5. Case Study

The Malin tunnel is located in Wudang District, Guiyang City. It is a separated two-way six-lane tunnel. The inner outline is a three-center round curved side wall structure. The net area is 123.68 m^2, the net span is 17.61 m, the net height is 5.0 m, and the flatness ratio is 0.618 (as shown in Figure 8). The designed speed of 100 km/h is tailored, as that

Table 11: Stability index value and bench division of tunnel drift.

Description of tunnel stability	Basically stable	Very stable	Highly stable
Bench division	Bench division is necessary and temporary invert should be adopted	Bench division is necessary and temporary invert is not compulsive	Bench division is unnecessary

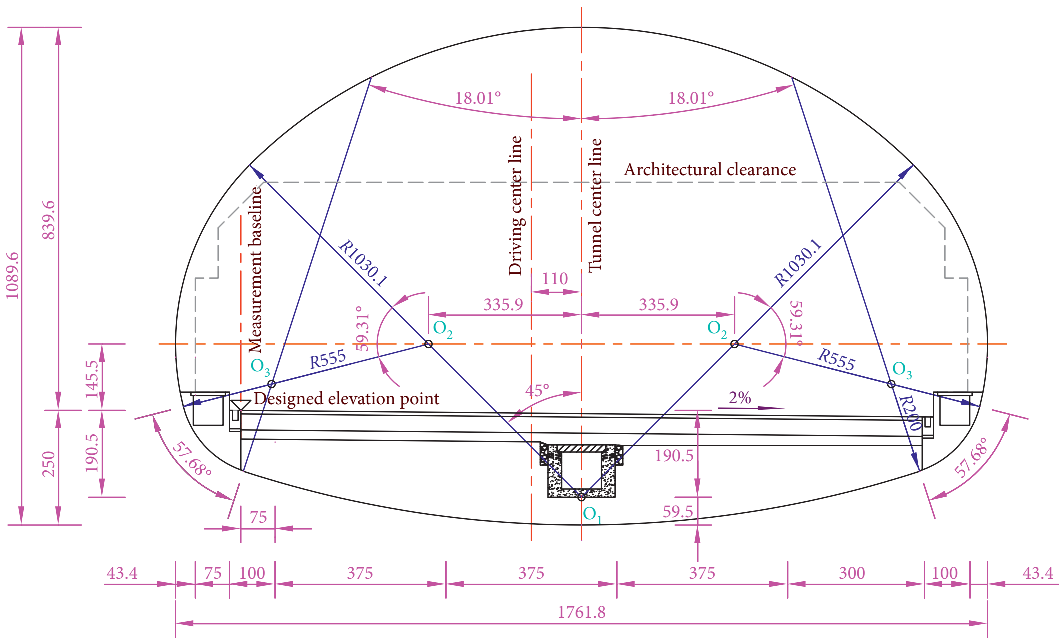

Figure 8: Inside outline of Malin tunnel.

Table 12: Calculation results of Malin tunnel construction method.

Item	Quantitative index
One-step span	15.9
Overall span	19.9
Number of calculated lateral drift	1.2
Number of determined lateral drift	2.0
Determined one-step excavation span	9.94
Index of surrounding rock stability F	27.81
Stability of surrounding rock	Very stable
Recommended method	CD method

Figure 9: Photo of CD method construction in Malin tunnel.

of expressway. The total length of the left tunnel is 745 m, the total length of the right tunnel is 760 m, and the maximum buried depth of the tunnel is about 98.7 m.

The surrounding rock is mainly composed of full-moderately weathered dolomite and dolomitic limestone. The rock grades mainly fall into grade IV and grade V. The grade V surrounding rock is mainly gravel, highly weathered dolomitic limestone, and cataclasite. The self-stability of surrounding rock is poor, so it is not controversial to use the double-side drift method for the grade V rock. Our method is applied to determine the construction method for the grade IV surrounding rock.

According to the survey and design of the Malin tunnel, the excavation span, rock strength, and rock integrity coefficient of grade IV rock are 19.54 m, 25.4 MPa, and 0.69, respectively. The calculation results based on our evaluation system are listed in Table 12.

Therefore, the grade IV surrounding rock section of the Malin tunnel should be constructed using the CD method with two lateral drifts in the cross section. The left and right drifts are divided into upper and lower drifts, and the tunnel construction is implemented with the CD method (Figure 9). The safety and efficiency of the construction process have been verified in the whole construction process.

6. Conclusions

In this paper, the orthogonal test method was used to establish a three-factor five-level test model, and the quantitative relationship functions between the three factors and the stability of the surrounding rock of the tunnel were given. The following conclusions can be drawn from this paper:

(1) The tunnel excavation span is negatively related to the stability of the surrounding rock of the tunnel, which can be described by a power function. The strength of the surrounding rock of the tunnel is positively related to the stability of the surrounding rock of the tunnel and can be described by a power function; the rock integrity coefficient is positively related to the stability of the surrounding rock of the tunnel, and their relationship can be described by a logarithmic function.

(2) An equation for determining the construction method of ultra-large-span tunnel is constructed, which can quantitatively reflect the contribution of excavation span of tunnel, the number of lateral drifts in cross section, surrounding rock strength, and rock integrity coefficient to surrounding rock stability of tunnel. The research results provide the theoretical basis for the identification and selection of construction method for ultra-large-span tunnel and provide theoretical calculation basis for determining the number of drifts in the cross section.

Data Availability

The data used to support the findings of this study are available from the corresponding author upon request.

Conflicts of Interest

The authors declare that they have no conflicts of interest regarding the publication of this paper.

Acknowledgments

This study was financially supported by the Special Science and Technology Innovation Fund of Research Institute of Highway Ministry of Transport (grant no. 2019-C505) and the Central Public-Interest Scientific Institution Basal Research Fund (grant no. 2020-9032).

References

[1] X. Chong-bang, Z.-G. Yang, and H. Wang, "Optimization analysis on construction method of shallow buried large section tunnel," *Highway*, vol. 61, no. 4, pp. 261–264, 2016.

[2] Y. Hong-wei and W. Wang, "Study of optimal proposal and field test for CRD excavation method of shallow-buried tunnel," *Journal of Railway Science and Engineering*, vol. 15, no. 6, pp. 1509–1515, 2018.

[3] W. Liang and M.-L. Huang, "Subsidence and deformation control of large-span tunnel in water-bearing unfavorable geological conditions with CRD method," *Chinese Journal of Rock Mechanics and Engineering*, vol. 26, no. 2, pp. 3738–3742, 2007.

[4] H. Ming-Qi, X.-L. Fu, and L. Yun-chao, "Study on stability control of large-section subsea tunnels in weak strata by CRD construction method," *Chinese Journal of Rock Mechanics and Engineering*, vol. 26, no. 2, pp. 3084–3089, 2007.

[5] Y.-L. Qi, M.-X. Tang, and H. Cao, "Simulation of CRD construction method in large-section shallowmining subsea tunnel," *Chinese Journal of Underground Space and Engineering*, vol. 10, no. 1, pp. 136–143, 2014.

[6] X. Shi, J. Zhang, and L. Bao-chen, "A study of the construction sequences of a large-Section shallow-buried unsymmetrical loading tunnel by the CRD Method," *Modern Tunnelling Technology*, vol. 52, no. 3, pp. 193–199, 2015.

[7] X. Chong-bang, C.-C. Xia, and H.-H. Zhu, "Optimum analysis for construction scheme of multiple-arch tunnel with eight traffic lanes," *Chinese Journal of Rock Mechanics and Engineering*, vol. 28, no. 1, pp. 17–26, 2009.

[8] G.-H Zhang, C. Li-Biao, and Q. Shi-Xiong, "On-site supervision measure and analysis of Damaoshan tunnels with large section and small clear-distance," *Rock and Soil Mechanics*, vol. 31, no. 2, pp. 489–496, 2010.

[9] C. Jian-xun, Y.-bin Luo, and Li Wan, "Research status and chal-lenges of highway tunnel with super long span," *Road Machinery & Construction Mechanization*, vol. 35, no. 6, pp. 36–44, 2018.

[10] L. Zhi-Qing, C.-L. Ding, and D. Shi-Xue, "Analysis on deformation characteristics of surrounding rock in large section shallow loess tunnels," *Chinese Journal of Underground Space and Engineering*, vol. 10, no. S1, pp. 1623–1628, 2014.

[11] L. I. Xin-Zhi, L. I. Shu-Cai, and L. I. Shu-Chen, "Ground settlement deformation characteristic study of shallow large-span tunnel in construction process," *Chinese Journal of Rock Mechanics and Engineering*, vol. 30, no. S1, pp. 3348–3353, 2011.

[12] C. Zuo-Qiang, L. Rui-Hui, and C. Yao, "Study on transformation method of construction method for super-long span

highway tunnel," *Science Technology and Engineering*, vol. 20, no. 17, pp. 7059–7065, 2020.

[13] L. Yan-Yan, Y.-R. Zheng, and N. Kang, "Sensitivity analysis on influencing factors of tunnel stability," *Chinese Journal of Underground Space and Engineering*, vol. 11, no. 2, pp. 491–498, 2015.

[14] C.-C. Xia, C. Xiao-xiang, and X. Chong-bang, "Fine description of rock joint combined with block theory and its applications in extra-large cross-section multiple-arch tunnel," *Chinese Journal of Rock Mechanics and Engineering*, vol. 29, no. 1, pp. 13–20, 2010.

[15] Z. C. Tang, Q. Z. Zhang, and J. Peng, "Effect of thermal treatment on the basic friction angle of rock joint," *Rock Mechanics and Rock Engineering*, vol. 53, no. 4, pp. 1973–1990, 2020.

[16] J. Zou, Y.-Y. Jiao, Z. Tang, Y. Ji, C. Yan, and J. Wang, "Effect of mechanical heterogeneity on hydraulic fracture propagation in unconventional gas reservoirs," *Computers and Geotechnics*, vol. 125, Article ID 103652, 2020.

[17] Z. C. Tang and Y. Y. Jiao, "Choosing appropriate appraisal to describe peak spatial features of rock joint profiles," *International Journal of Geomechanics*, vol. 20, no. 4, Article ID 4020021, 2020.

[18] Z. C. Tang and Q. Z. Zhang, "Elliptical Hertz-based general closure model for rock joints," *Rock Mechanics and Rock Engineering*, vol. 55, no. 4, pp. 1945–1956, 2020.

[19] Z. C. Tang, L. Li, X. C. Wang, and J. P. Zou, "Influence of cyclic freezing-thawing on shear behaviors of rock fracture," *Cold Regions Science and Technology*, vol. 181, Article ID 103192, 2020.

[20] H. Hong-Xing, "The influence of excavation method on the stability of surrounding rock in mountain tunnel with rich water," *Journal of Water Resources and Architectural Engineering*, vol. 18, no. 3, pp. 150–155, 2020.

[21] X.-M. Han, M.-L. Sun, and L. Wen-Jiang, "Optimization of section shape and support parameters of tunnel under complicated conditions," *Rock and Soil Mechanics*, vol. 32, no. 1, pp. 725–731, 2011.

[22] CCCC Second Highway Consultants Co., Ltd., *Guidelines for Design of Highway Tunnels: JTG/T D70-2010*, China Communications Press, Beijing, China, 2010.

[23] R. Lu-Quan, *Regression Design and its Optimization*, Science Press, Beijing, China, 2009.

[24] F. Kai-Tai and M. Chang-Xing, *Orthogonal and Uniform Experimental Design*, Science Press, Beijing, China, 2001.